Ann. Geophys., 29, 1331–1340, 2011
www.ann-geophys.net/29/1331/2011/
doi:10.5194/angeo-29-1331-2011

Annales Geophysicae

The correlation between solar and geomagnetic activity – Part 1: Two-term decomposition of geomagnetic activity

Z. L. Du

Key Laboratory of Solar Activity, National Astronomical Observatories, Chinese Academy of Sciences, Beijing 100012, China

Received: 30 November 2010 – Revised: 29 May 2011 – Accepted: 17 July 2011 – Published: 5 August 2011

Abstract. By analyzing the logarithmic relationship between geomagnetic activity as represented by the annual *aa* index and solar magnetic field activity as represented by the annual sunspot number (R_z) during the period 1844–2010, *aa* is shown to lie in between two lines defined solely by R_z. Two ways can be used to decompose the *aa* index into two components. One is decomposing *aa* into the sum of the baseline (aa_b) and the remainder (aa_u) with a null correlation. Another is dividing the top-line (aa_t) into the sum of *aa* and the remainder (aa_d) with a null correlation. The first decomposition is similar to the traditional one. The second decomposition implies a nonlinear relationship of *aa* with R_z (aa_t) and a decay process (aa_d). Therefore, $aa_t = aa + aa_d = aa_b + aa_u + aa_d$: (i) aa_t is related to the solar energy potential of generating geomagnetic activity (associated with R_z); (ii) aa_b is related to transient phenomena; (iii) aa_u is related to recurrent phenomena; and (iv) aa_d is related to the energy loss in the transmission from solar surface to the magnetosphere and ionosphere that failed to generate geomagnetic activity.

Keywords. Magnetospheric physics (Solar wind-magnetosphere interactions)

1 Introduction

Since Mayaud (1972) designed the geomagnetic activity *aa* index from the 3-hourly K indices at two near-antipodal mid-latitude stations, numerous authors have used it to analyze the global geomagnetic activity and its correlation with solar activity (Schatten et al., 1978; Feynman, 1982; Legrand and Simon, 1989a; Nevanlinna and Kataja, 1993; Lukianova et al., 2009; Du et al., 2009; Du, 2011a). The *aa* index appears an 11-year cycle similar to that of sunspot activity, as described by the Zurich sunspot number (R_z). Studying the relationship between geomagnetic activity, as represented by *aa*, and solar activity, as represented by R_z, may contribute to understanding the origin and formation of the former.

Geomagnetic activities have long been known to be correlated with solar activities (Snyder et al., 1963; Russell and McPherron, 1973; Garrett et al., 1974; Feynman and Crooker, 1978). Geomagnetic activities can be resulted from variable current systems formed in the magnetosphere and ionosphere, such as the ring current and auroral ionospheric current, which are strongly modulated by solar activities via the interaction of the magnetosphere with solar winds (Feynman, 1980; Legrand and Simon, 1989a,b; Demetrescu and Dobrica, 2008) or others (Legrand and Simon, 1981, 1989a; Stamper et al., 1999; Tsurutani et al., 2006). It is believed that the geomagnetic activity is well associated with the solar wind speed (V), the southward component (B_z) of the interplanetary magnetic field (IMF) and their product (Snyder et al., 1963; Russell and McPherron, 1973; Garrett et al., 1974; Crooker et al., 1977; Svalgaard, 1977; Feynman, 1980; Wang and Sheeley, 2009). In general, the magnetosphere exhibits approximately a linear response to the solar wind drivers. However, a nonlinear behavior is significant in the declining phase of a solar cycle, which is related to increased solar wind speeds (Legrand and Simon, 1989a,b; Venkatesan et al., 1991; Echer et al., 2004; Johnson and Wing, 2005).

The geomagnetic activity results from two main solar sources (Legrand and Simon, 1981; Venkatesan et al., 1982; Feynman, 1982; Legrand and Simon, 1989a,b; Gonzalez et al., 1990; Venkatesan et al., 1991; Echer et al., 2004). The first source is related to transient phenomena such as solar flares, prominence eruptions, and coronal mass ejections (CMEs), and follows the sunspot cycle (Venkatesan et al., 1991). The second source is related to recurrent phenomena (high-speed solar wind streams) and tends to peak in

Correspondence to: Z. L. Du
(zldu@nao.cas.cn)

Published by Copernicus Publications on behalf of the European Geosciences Union.

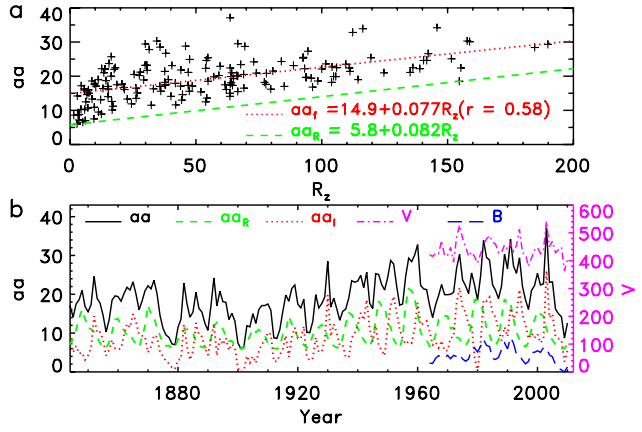

Fig. 1. **(a)** Scatter plot of aa against R_z (pluses), linear fit (dotted), and baseline aa_R (dashed). **(b)** The time series of aa (solid), aa_R (dashed) from Eq. (2) and aa_I (dotted) from Eq. (3) since 1844. The time series of V (dash-dotted) and B (long-dashed) since 1964 are also shown for comparison, with the B values so scaled that they can be clearly seen.

the declining phase or at the solar minimum of the cycle (Legrand and Simon, 1981; Venkatesan et al., 1982; Legrand and Simon, 1989a,b; Tsurutani et al., 2006). Feynman (1982) analyzed the relationship between the annual aa and R_z series from 1869 to 1975 and found that the aa values are all above a base line (aa_R) that is linearly related to R_z. Then, she decomposed the aa index into two equally strong periodic components: aa_R and the remainder $aa_I = aa - aa_R$. The first one (the "short lived" R component) is associated with the transient phenomena and follows the sunspot cycle, while the second one (the "slowly varying" interplanetary I component) is associated with the recurrent phenomena and is almost 180° out of phase with the sunspot cycle (Hathaway and Wilson, 2006). Legrand and Simon (1989a) classified the geomagnetic activity in four classes: the magnetic quiet activity, the recurrent activity, the fluctuating activity, and the shock activity. At mid-latitude, the geomagnetic activity is sensitive both to the auroral phenomena (particle precipitations, substorms, and auroras) which are at the origin of the auroral electrojet (AE) activity, and to the equatorial ring current which is the source of the geomagnetic storms (Legrand and Simon, 1989a,b). Therefore, the aa index is an integral effect of various sources of geomagnetic activity.

The relationship between the solar and geomagnetic activity is not a simple linear one (Feynman, 1983; Legrand and Simon, 1983) due to various sources of geomagnetic activity. Decomposing the geomagnetic activity (aa index) into different parts may help understand its origins.

In this paper, we first reexamine the work of Feynman (1982) to decompose the annual aa index for the data available (Sect. 2) into two components based on a linear relationship between aa and R_z (Sect. 3). To elucidate how aa depends on R_z, we analyze the scatter plot of $\mathbf{ln}aa$ against $\mathbf{ln}R_z$ in Sect. 4. All the data points are found to be in between the two lines of baseline ($\mathbf{ln}aa_b$) and top-line ($\mathbf{ln}aa_t$). According to the baseline, the aa index can be decomposed into two components: aa_b and the remainder $aa_u = aa - aa_b$ with a null correlation (Sect. 4.1). This decomposition is similar to that of Feynman (1982), but the relationship between aa_b and R_z is nonlinear. The top-line provides another way to decompose aa_t into two components: aa and $aa_d = aa_t - aa$ with a null correlation (Sect. 4.2). We attempt to explain the second decomposition by a nonlinear model (Sect. 4.2.1) and a decay process (Sect. 4.2.2). The aa index is the remainder of aa_t after decay aa_d. Some conclusions are discussed and summarized in Sect. 5.

2 Data

To suppress the high frequencies involved in the solar rotation and seasonal variations, in this study the geomagnetic activity is represented by the annual averages of aa index (Mayaud, 1972) using reliable values since 1868[1] and the equivalent ones from measurements in Finland from 1844 to 1867 (Nevanlinna and Kataja, 1993). The solar (magnetic field) activity is represented by the annual averages of R_z[2] from 1844 to 2010. In addition, for comparison we use the annual speed (V) and magnetic field (B) of solar wind from the OMNI data sets since 1964[3], and the Dst (disturbance storm time)[4] index representing the ring current (Gonzalez et al., 1990) since 1958.

3 Two-term decomposition of aa according to the linear relationship between aa and R_z

In this section, we repeat the Feynman (1982) work to decompose aa into two components, using the data from 1844 to 2010. Figure 1a shows the scatter plot of aa against R_z (pluses). The dotted line indicates the linear fit of aa to R_z, with the regression equation given by

$$aa = 14.9 + 0.077 R_z. \quad (1)$$

It is seen that the data points are all above the (dashed) baseline, defined by the lower envelope,

$$aa_R = 5.8 + 0.082 R_z. \quad (2)$$

The remainder of aa is then

$$aa_I = aa - aa_R. \quad (3)$$

Figure 1b shows the time series of aa (solid), aa_R (dashed), and aa_I (dotted) since 1844. The correlation coefficient between the two components, aa_R and aa_I, is almost zero

[1] ftp://ftp.ngdc.noaa.gov/STP/SOLAR_DATA/RELATED_INDICES/AA_INDEX/

[2] http://www.ngdc.noaa.gov/stp/spaceweather.html

[3] ftp://nssdcftp.gsfc.nasa.gov/spacecraft_data/omni/

[4] http://www.ngdc.noaa.gov/stp/spaceweather.html

Table 1. Correlation coefficients (r) between aa, R_z, aa_R, aa_I, V, and B.

r	aa	$aa_R(R_z)$	aa_I	V	B
aa	1	0.58	0.79	0.74	0.83
$aa_R(R_z)$		1	−0.05	−0.06	0.78
aa_I			1	0.84	0.31
V				1	0.32

($r = -0.05$), implying that aa_I has a 90° (~3-yr) rather than a 180° (Feynman, 1982; Li, 1997; Hathaway and Wilson, 2006) phase shift to aa_R. The phase shift is related to the time delay of aa to R_z (Echer et al., 2004; Du, 2011b). Figure 1b also shows V (dash-dotted) and B (long-dashed) since 1964 for comparison. The correlation coefficients between these parameters are listed in Table 1.

One sees in Table 1 that: (i) aa is positively correlated with R_z ($r = 0.58$), aa_R ($r = 0.58$), aa_I ($r = 0.79$), V ($r = 0.74$), and B ($r = 0.83$); (ii) $aa_R(R_z)$ is well correlated with B ($r = 0.78$) but has a null correlation with V ($r = -0.06$); and (iii) aa_I has a much higher correlation with V ($r = 0.84$) than with B ($r = 0.31$). Therefore, aa_R and aa_I are well associated with B and V, respectively.

The two components of aa_R and aa_I have been explained by two main solar sources of geomagnetic activity (Legrand and Simon, 1981; Venkatesan et al., 1982; Legrand and Simon, 1989a; Gonzalez et al., 1990; Venkatesan et al., 1991; Legrand and Simon, 1989a,b; Echer et al., 2004): (i) aa_R is related to solar flares and coronal mass ejections (CMEs); and (ii) aa_I is related to high-speed solar wind streams and is out of phase with the sunspot cycle (Feynman, 1982).

4 Two-term decomposition of aa according to the logarithmic relationship between aa and R_z

To elucidate how aa depends on R_z, we analyze the correlation between the *natural logarithms* of the annual aa and R_z from 1844 to 2010. The scatter plot of $\mathbf{ln}aa$ against $\mathbf{ln}R_z$ is shown in Fig. 2. The dotted line indicates the linear fit of $\mathbf{ln}aa$ to $\mathbf{ln}R_z$, with the regression equation given by

$$\mathbf{ln}aa = 2.13 + 0.21\mathbf{ln}R_z, \quad \text{or} \quad aa = 8.41R_z^{0.21}. \tag{4}$$

The positive correlation between $\mathbf{ln}aa$ and $\mathbf{ln}R_z$ ($r = 0.67$) is stronger than that between aa and R_z ($r = 0.58$), implying that aa varies preferably nonlinearly with R_z. Also shown in the figure are the years of the maximum (triangles) and minimum (circles) amplitudes of the sunspot cycle.

One very prominent property in Fig. 2 is that the data points are all in between the two parallel (dashed) lines with

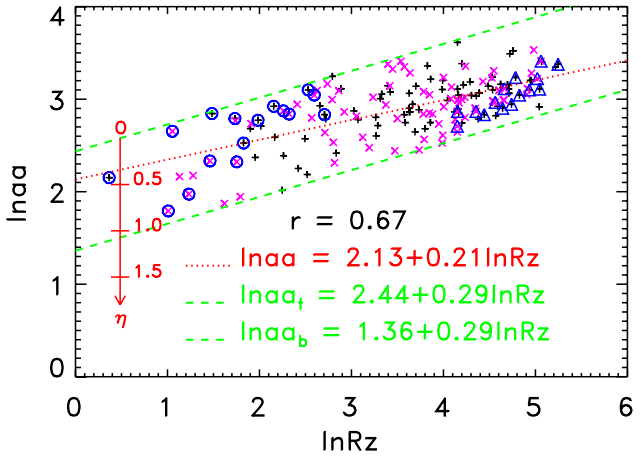

Fig. 2. Scatter plot of $\mathbf{ln}aa$ against $\mathbf{ln}R_z$ (black pluses for odd-numbered cycles and purple crosses for even-numbered cycles) with a correlation coefficient of $r = 0.67$. The dotted line indicates the linear fit of $\mathbf{ln}aa$ to $\mathbf{ln}R_z$. The data points are all in between the two parallel (dashed) lines of $\mathbf{ln}aa_t$ (top) and $\mathbf{ln}aa_b$ (base). Triangles and circles denote the years of the maximum and minimum amplitudes of the sunspot cycle, respectively. The coordinate axis η describes decay strength.

their equations defined (from two points on baseline or topline) by

$$\mathbf{ln}aa_b = 1.36 + 0.29\mathbf{ln}R_z, \quad \text{or} \quad aa_b = e^{1.36}R_z^{2/7} \tag{5}$$

and

$$\mathbf{ln}aa_t = 2.44 + 0.29\mathbf{ln}R_z, \quad \text{or} \quad aa_t = e^{2.44}R_z^{2/7}. \tag{6}$$

The above equations suggest that a certain level of solar activity (R_z) is associated with at least (most) aa_b (aa_t) of the geomagnetic activity. From aa_b and aa_t, two new indices, aa_u and aa_d, can be defined such that

$$aa = aa_b + aa_u, \quad \text{or} \quad aa_u = aa - aa_b \tag{7}$$

and

$$aa_t = aa + aa_d, \quad \text{or} \quad aa_d = aa_t - aa. \tag{8}$$

The null correlation of aa_b with aa_u ($r = 0.09$) implies that aa can be decomposed into two independent components: aa_b and aa_u. Similarly, the null correlation of aa with aa_d ($r = -0.0003$) implies that aa_t can be divided into two independent orthogonal terms: aa and aa_d.

As aa_b and aa_t are strictly defined by Eqs. (5)–(6), the correlation coefficient of $\mathbf{ln}aa_b$ or $\mathbf{ln}aa_t$ with $\mathbf{ln}R_z$ is one, having the same periodicity, phase, and relative amplitude, so that aa_b (aa_t) follows R_z ($r = 0.94$) well. If aa were proportional to aa_b (aa_t), the remainder aa_u (aa_d) would be random. However, the correlation of aa_u with aa ($r = 0.84$) is stronger than that of aa_b with aa ($r = 0.62$), and the correlation of aa_d with aa_t ($r = 0.78$) is stronger than that of aa

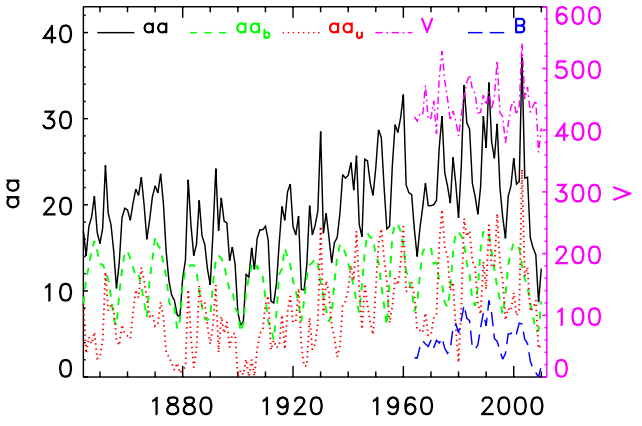

Fig. 3. Time series of aa (solid), aa_b (dashed) from Eq. (5), aa_u (dotted) from Eq. (7), V (dash-dotted), and B (long-dashed), with the B values so scaled that can be clearly seen.

with aa_t ($r = 0.62$), Therefore, some underlying information must exist in both aa_u and aa_d.

The strong correlation of aa_d with R_z ($r = 0.75$) and the null correlation of aa_d with aa ($r = 0.00$) imply that aa_d is well associated with the level of R_z (solar activity). In contrast, the strong correlation of aa_u with aa ($r = 0.84$) and the null correlation of aa_u with R_z ($r = 0.07$) imply that aa_u reflects the variation in aa (geomagnetic activity).

4.1 Two-term decomposition of *aa* based on the baseline

Similar to Sect. 3, one decomposition method of the aa index is according to the baseline (aa_b), as the aa values are all above aa_b (Fig. 2). Figure 3 shows the two components, aa_b (dashed) from Eq. (5) and aa_u (dotted) from Eq. (7), together with aa (solid), V (dash-dotted), and B (long-dashed) for comparison. The correlation coefficients between these parameters are listed in Table 2.

The following may by noted in Table 2: (i) aa is positively correlated with aa_b, aa_u, V, and B; (ii) aa_b is well correlated with B ($r = 0.83$) but has a null correlation with V ($r = 0.03$); and (iii) aa_u has a much higher correlation with V ($r = 0.85$) than with B ($r = 0.41$). Therefore, aa_b and aa_u are well associated with B and V, respectively, reflecting the two sources of geomagnetic activity.

This decomposition is similar to that in Sect. 3. The aa_b and aa_u terms in this section correspond similarly to the R and I components in the previous section, respectively. The main discrepancy is that the R component is linearly related to R_z (Eq. 2), while aa_b is related to R_z in the form of a power-law (Eq. 5). Thus, the aa_b component can be explained to be nonlinearly related to solar flares and CMEs, and the aa_u component is related to high-speed solar wind streams having a 90° (∼3-yr) phase shift to aa_b.

It should be pointed out in Fig. 2 that there is a maximum (aa_t) for the aa values and that there is a maximum

Table 2. Correlation coefficients between aa, aa_b, aa_u, V and B.

r	aa	aa_b	aa_u	V	B
aa	1	0.62	0.84	0.74	0.83
aa_b		1	0.10	0.03	0.83
aa_u			1	0.85	0.41

($aa_t - aa_b$) for the aa_u component, which is part of aa above the baseline aa_b (Eq. 7). This result suggests that R_z is associated with a certain amount of solar energy (E_t) potential of generating geomagnetic activity (aa) whose maximum (aa_t) is related to E_t. The energy (E_t) consists of three parts: (i) the first part (E_b), being related to the transient phenomena, generates the geomagnetic activity (aa_b) that is well associated with R_z ($aa_b \propto R_z^{2/7}$); (ii) the second part (E_u), being related to the recurrent phenomena, generates the geomagnetic activity (aa_u) that is almost uncorrelated with the former (aa_b); and (iii) the third part ($E_d = E_t - E_b - E_u$), generating no geomagnetic activity, might be interpreted as the energy loss in the energy transmission from solar surface to the magnetosphere and ionosphere, which may involve very complex processes (see also Sect. 4.2 and Discussion) and may be related to the time delay of geomagnetic activity (aa) to solar activity (R_z).

For the decomposition in Fig. 2, the aa values are all above the baseline aa_R (Eq. 2), while there seems to be no upper limit for the aa or aa_I (Eq. 3) values shown in Fig. 1a – at least such a limit (if existing) is not apparent.

4.2 Two-term decomposition of *aa* based on the top-line

Another alternate decomposition method is by use of the top-line (aa_t), as the aa values are all below aa_t (Fig. 2). The two components, aa and aa_d from Eqs. (6) and (8), have a null correlation ($r \sim 0$), implying that the aa index has a 90° (∼ 3-yr) phase shift to aa_d. This decomposition might be explained by a nonlinear model and a decay process.

4.2.1 A nonlinear model

Suppose that the variation rate of aa is proportional to that of R_z,

$$\frac{\Delta aa}{aa} \propto \frac{\Delta R_z}{R_z}, \quad \text{or} \quad \frac{\partial aa}{\partial R_z} = \gamma \frac{aa}{R_z}, \tag{9}$$

where γ is called "response efficiency" of aa to R_z. The solution to this equation is in the form of

$$\mathbf{ln} aa = \beta + \gamma \mathbf{ln} R_z, \quad \text{or} \quad aa(R_z) = e^{\beta} R_z^{\gamma}, \tag{10}$$

where β is an integral constant. Thus, Eq. (10) can be taken as a general form of Eqs. (5)–(6) for

$$\begin{aligned} \gamma &= 2/7, \\ \beta_t &= 2.44, \\ \beta_b &= 1.36. \end{aligned} \tag{11}$$

It suggests from Eqs. (10) and (4) that aa varies with R_z nonlinearly rather than linearly. In fact, the values of γ for the top- and base-line are not strictly equal to one another. By carefully examining the top-line in Fig. 2, two possible values of γ are $\gamma_t = 0.27$ and 0.31 (from two different pairs of the upper envelope), corresponding to $\beta_t = 2.49$ and 2.39, respectively. We have taken an average of $\gamma_t = 0.29$, which is equal to $\gamma_b = 0.29$ for the baseline, and $\beta_t = 2.44$ correspondingly. Therefore, γ and β have uncertainties of about $\Delta\gamma = 0.02$ and $\Delta\beta = 0.05$, respectively. The γ value reflects the generation efficiency of aa by solar (activity) energy that is related to R_z, only about 2/7 (29 %) of the relative variation in R_z being related to the variation in aa in terms of annual averages.

4.2.2 A decay process

From Eqs. (5), 6), and (11) we have

$$aa_b = e^{-(\beta_t - \beta_b)} aa_t = e^{-1.08} aa_t. \tag{12}$$

In accordance with this equation, all the data points in Fig. 2 can be divided into many groups, each lying on an oblique narrow stripe (belt) parallel to the top-line. These stripes are denoted by a coordinate axis (η).

Suppose that aa undergoes a decay process in terms of the variable z,

$$-\Delta aa \propto aa\Delta z, \quad \text{or} \quad \frac{\partial aa}{\partial z} = -\frac{1}{L} aa, \tag{13}$$

where L is the decay scale. Its solution is

$$aa(z) = e^{-z/L} aa_0, \tag{14}$$

where aa_0 is an integral constant. Because the aa values are all in between the two lines (Fig. 2), $z = 0$ can be taken as the top-line and $aa_0 = aa_t$ as the boundary condition, so that

$$aa(z) = \begin{cases} e^{-z/L} aa_t, & 0 \le z \le 1.08L, \\ aa_b, & z > 1.08L, \end{cases} \tag{15}$$

and the decay term is

$$\begin{aligned} aa_d(z) &= aa_t(z) - aa(z) \\ &= \begin{cases} (1 - e^{-z/L}) aa_t, & 0 \le z \le 1.08L, \\ aa_t - aa_b, & z > 1.08L. \end{cases} \end{aligned} \tag{16}$$

The above two equations can be easily explained if z is temporarily taken as a length variable with its origin at the "outer surface" of the magnetosphere and its positive direction towards the Earth. (i) At first, the interaction of solar activities (solar winds and CMEs, etc.) with the magnetosphere produces geomagnetic activity ($aa = aa_t$), which is the top-line in Fig. 2. Then aa_t undergoes a decay process according to $aa_d(z) = (1 - e^{-z/L}) aa_t$ for $0 \le z \le 1.08L$ as it attempts to go through the decay range (ionosphere as well as magnetosphere, hereafter DR, where aa decays). Only the remainder $aa(z) = aa_t - aa_d(z) = e^{-z/L} aa_t$ is observed after the DR. Various decays, due to various thicknesses and densities of the DR for different districts or different time periods (and different solar activities), constitute the randomly scattered points of aa in Fig. 2 (the random distribution of aa_d or aa is the cause of the null correlation between them). (ii) For $z > 1.08L$, aa has already passed over the DR and will not decay further. As the maximum decay in the whole DR is $\overline{aa}_d = aa_t - aa_b$, the minimum aa is then $\underline{aa} = aa_t - \overline{aa}_d = aa_b$, which is the baseline in Fig. 2.

It should be noted that the decay aa_d is well correlated with aa_t ($r = 0.78$) or R_z ($r = 0.75$), meaning that a higher level of R_z tends to be associated with a larger aa_d or z. Although a stronger (weaker) solar activity R_z (corresponding to the energy E_t) is related to a higher (lower) level of aa_t, more (less) decays (or the "energy loss" E_d) will also be produced while transmitting through the DR. When aa has finally passed over the DR, only a part is left: the observed $aa = aa_t - aa_d$ (or the energy $E = E_t - E_d$). Thus, the variable z is in fact a quantity to describe the decay strength (or the energy loss E_d) in the DR, and L is the decay scale (or the maximum energy loss $E_{d,max}$). The z/L value reflects the energy loss rate ($E_d/E_{d,max}$), which is related to the intensity and orientation of the solar dipole (Simon and Legrand, 1989), the topology and density (especially the ion density) of the DR, the size and shape of the current sheet, or the ion inertial scale (Leamon et al., 2000; Matthaeus et al., 2008). The formation is related to the interaction mechanism of solar activities (solar winds and CMEs, etc.) with the magnetosphere (and of the fast with slow solar winds) and the state (strength, velocity, and direction) of the solar wind. More geomagnetic activities can be produced if the solar wind reaches the magnetosphere perpendicularly than in any other direction.

This explanation is, of course, a simplified characterization. In fact, the geomagnetic activity may be produced and decayed all the way from the magnetosphere to the Earth. Magnetic fields play a determining role in the formation and dynamics of solar activities. Besides sunspots (R_z), the magnetic fields also produce other phenomena of solar activities, such as solar flares, prominence eruptions, energetic protons, CMEs, and solar winds (Legrand and Simon, 1989a), in nonlinear processes more or less similar to Eq. (15). As the source activities of geomagnetic activity, these activities have already undergone decays before arriving at the magnetosphere (e.g., in solar corona), and play a role of mid-processes from the solar magnetic field activity to geomagnetic activity (see Discussions). From the perspective of the overall result, the formation of aa can be totally expressed

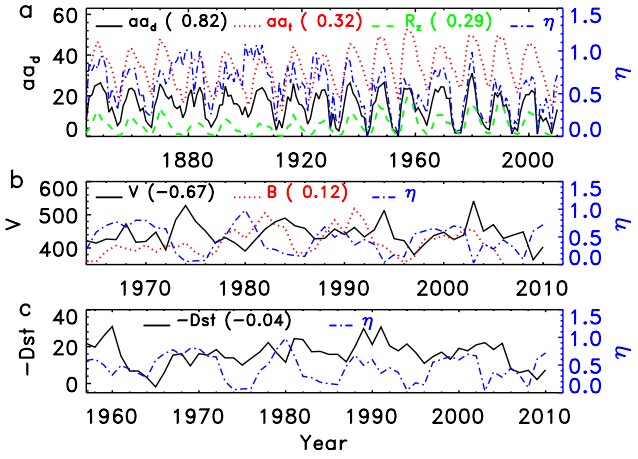

Fig. 4. **(a)** aa_d (solid) from Eq. (8), aa_t (dotted) from Eq. (6) and R_z (dashed) since 1844. **(b)** V (solid), B (dotted), and η (dash-dotted) since 1964. **(c)** −Dst (solid) and η (dash-dotted) since 1958. The values of R_z and B are so scaled that they can be clearly seen. The numbers in brackets indicate the correlation coefficients of the parameters with η.

as aa_t in Eq. (6), and the decay process can be described by Eq. (16).

4.2.3 *aa*'s expression and decay index η

Combining Eq. (6) with Eq. (15), all the aa values can be mathematically expressed as

$$aa = e^{2.44-\eta} R_z^{2/7} \quad (0 \le \eta \le 1.08), \tag{17}$$

where

$$\eta = z/L \tag{18}$$

is called "decay index": the quantity of z normalized to L (Fig. 2), which is related to the decay rate, $aa_d/aa_t = 1 - e^{-\eta}$. Implied in Eq. (17) is that the geomagnetic activity is generated via a nonlinear relationship with R_z as $R_z^{2/7}$ and a decay process according to $e^{-\eta}$.

To study the property of η, its value can be calculated by Eq. (17),

$$\eta = 2.44 + (2/7)\mathbf{ln}R_z - \mathbf{ln}aa. \tag{19}$$

Figure 4a shows the time series of aa_d (solid), aa_t (dotted), R_z (dashed), and η (dash-dotted) for comparison.

It is apparent in Fig. 4a that a larger η corresponds to more decays (aa_d) and almost, but not quite, a higher R_z. In contrast, a smaller η (solid) corresponds to less decays and almost, but not quite, a lower R_z. The η values at the years of solar minima are much more scattered (circles in Fig. 2), ranging from 0.02 to 0.94 with an average of $\overline{\eta}_{min} = 0.36$, while those at the years of solar maxima (triangles) are more concentrated, ranging from 0.50 to 0.94 with an average of $\overline{\eta}_{max} = 0.76$. This may be the reason why the dynamics of the magnetosphere tends to be more linear at maximum than at minimum (Johnson and Wing, 2005). The larger values of η at solar maxima than at solar minima ($\overline{\eta}_{max} > \overline{\eta}_{min}$) can explain the following phenomenon. The aa index at a higher R_z (around the maximum) tends to undergo more decays and for a longer time when going through the DR, leading to a longer lag time of aa to R_z at a maximum rather than at a minimum (Wang and Sheeley, 2009; Wilson, 1990; Du, 2011b,c).

Table 3. Correlation coefficients between aa, aa_t, aa_d, η, V, B, and Dst.

r	aa	aa_t	aa_d	η	V	B	Dst
R_z	0.58	0.95	0.75	0.29	−0.06	0.78	−0.64
aa	1	0.62	0.00	−0.52	0.74	0.83	−0.80
aa_t		1	0.78	0.32	0.03	0.83	−0.68
aa_d			1	0.82	−0.48	0.41	−0.27
η				1	−0.67	0.12	0.04
V					1	0.32	−0.37
B						1	0.16

In Fig. 2, the $\mathbf{ln}aa$-$\mathbf{ln}R_z$ data pairs are divided into two parts: one is related to odd-numbered cycles (pluses) and another is related to even-numbered cycles (crosses). The average decay index η (0.57) for odd-numbered cycles is slightly less than that (0.59) for even-numbered cycles, which may be related to the stronger correlation for odd-numbered cycles than for even-numbered cycles (Du, 2011b,c).

4.2.4 The correlations of η with V, B, and Dst

Figure 4b shows the time series of V (solid), B (dotted), and η (dash-dotted) for comparison. One can see that η is negatively correlated with V ($r = -0.67$) and almost independent of B ($r = 0.12$), implying that solar winds with lower speeds tend to decay more. This means that one usually analyzes the correlation between geomagnetic activity and the solar wind speed above a certain value.

Figure 4c shows the Dst index (solid) and η (dash-dotted) for comparison. It is seen that η is almost independent of Dst ($r = 0.04$). One possible reason is that Dst is well anti-correlated with aa ($r = -0.8$), while aa has a null correlation with aa_d ($r = 0.00$). The correlation coefficients involved in these parameters are summarized in Table 3.

It should be pointed out in Table 3 that η is well correlated with aa_d ($r = 0.82$), negatively correlated with V ($r = -0.67$) or aa ($r = -0.52$), weakly correlated with R_z or aa_t ($r \sim 0.3$), and almost uncorrelated with B or Dst ($r \sim 0$). Therefore, the decay index (η) is mainly related to the solar wind speed (V). The reason may be due to that: (i) the (average) speed of solar wind is slower than that of the transient phenomena (e.g., CMEs); (ii) only part of the solar wind energy is transmitted to geomagnetic activity in the interaction with the magnetosphere, which spends time; and (iii) the

slower solar wind plasma is more difficult to transmit the magnetosphere and decays more than the faster one.

5 Discussions and conclusions

By analyzing the relationship between $\mathbf{ln}aa$ and $\mathbf{ln}R_z$, this study shows that the aa values are all in between the two lines of $aa_t = e^{2.44} R_z^{2/7}$ and $aa_b = e^{1.36} R_z^{2/7}$ defined solely by R_z. According to the two lines, two ways can be selected to divide the aa index into two components. If one is chosen as the baseline aa_b similar to the R component used by Feynman (1982), the remainder $aa_u = aa - aa_b$ (part of aa above aa_b) will have a null correlation with the former ($r = 0.09$), implying an independent decomposition. On the other hand, if one is chosen as the top-line aa_t, the "minus remainder" $aa_d = -(aa - aa_t)$ will well follow the former ($r = 0.78$). The second decomposition is equivalent to dividing aa_t into two terms of aa and aa_d (part of aa_t above aa) with a null correlation ($r = 0.00$). With this decomposition, the aa_t term is interpreted as a nonlinear relation of aa with R_z and aa_d as a decay in transmission (due to energy loss). All the aa indices can be mathematically expressed as $aa = e^{2.44\pm0.05-\eta} R_z^{2/7\pm0.02}$ for $0 \le \eta \le 1.08$. The decay index η is mainly modulated by the solar wind speed V ($r = -0.67$), and is almost independent of both the magnetic field B of solar wind and the Dst index (ring current), as can be seen in Table 3 and Fig. 4.

The aa_b and aa_u terms in this study correspond similarly to the R and I components, respectively, with the main discrepancy that the R component is linearly related to R_z (Eq. 2), while aa_b is related to R_z in the form of a power-law (Eq. 5). The aa_u or aa_I (part of aa above aa_R) component tends to have a 90° (~3-yr) rather than a 180° phase shift relative to aa_b or R_z (Fig. 3), so that the correlation coefficient between aa_b and aa_u is close to zero ($r = 0.09$).

To demonstrate the period in aa_u, we obtain from Eqs. (5)–(8), (15), and (18),

$$\begin{aligned} aa &= aa_t - aa_d(\eta) = e^{1.08-\eta} aa_b, \\ aa_u(\eta) &= aa - aa_b \quad\;\; = \left(e^{1.08-\eta} - 1\right) aa_b. \end{aligned} \tag{20}$$

Therefore, (i) the reason for the periodic variation in aa_u (or aa_I) is only due to the periodic aa_b even if η is not a constant. (ii) The reason for the 90° phase shift of aa_u to aa_b is as follows. The recurrent geomagnetic activity is prevalent throughout the declining phase of the cycle (Wang and Sheeley, 2009), which may be related to the irregularity of the decay processes. The lag time of aa to R_z and the decay time contribute a phase ϕ to $aa_u(\eta)$ such that $\eta = \eta' + i\phi$, where i is the imaginary unit. The phase ϕ has an average of about $\overline{\phi} = \pi/2$ in the almost randomly distributed range of $[0, \pi]$. Thus, the correlation coefficient between aa_b and aa_u is close to zero (because the correlation coefficient between $\sin(t)$ and $\sin(t + \pi/2)$ is zero).

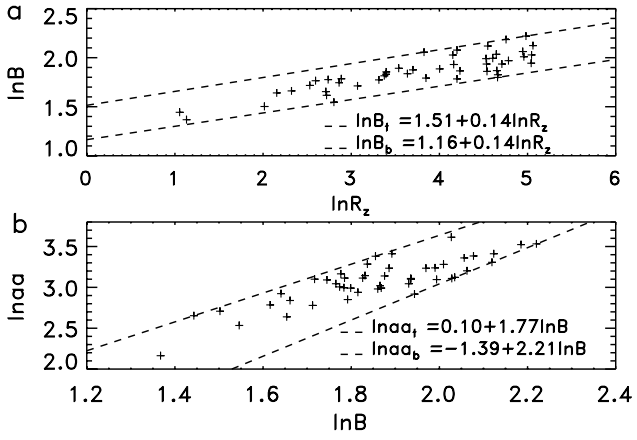

Fig. 5. **(a)** Scatter plot of $\mathbf{ln}B$ against $\mathbf{ln}R_z$ (pluses). The data points are all in between the two parallel (dashed) lines of $\mathbf{ln}B_t$ (top) and $\mathbf{ln}B_b$ (base). **(b)** Scatter plot of $\mathbf{ln}aa$ against $\mathbf{ln}B$ (pluses). The data points are all in between the two (dashed) lines of $\mathbf{ln}aa_t$ (top) and $\mathbf{ln}aa_b$ (base).

The fact that there are more decays at solar maxima than at solar minima is related to or can explain (partly) the following phenomena. (i) The "pearls" of ~ 1-year pulsations in B_z are less near the maxima (Papitashvili et al., 2000). (ii) There is more mixing of fast and slow solar wind plasma at a solar maximum (Bame et al., 1976; Tu and Marsch, 1995; Richardson et al., 2000). (iii) The intensity of galactic cosmic rays (GCR) is reversely correlated with R_z (Nagashima et al., 1991; Stamper et al., 1999). (iv) The geomagnetic activity lags behind the solar activity for a longer time at a solar maximum than at a solar minimum (Legrand and Simon, 1981; Wang and Sheeley, 2009; Wilson, 1990; Du, 2011b,c). (v) Some activities may have stronger correlations with R_z around solar maxima than around solar minima.

It is well known that there are two main solar sources of geomagnetic activity (Legrand and Simon, 1981; Venkatesan et al., 1982; Feynman, 1982; Legrand and Simon, 1989a,b; Gonzalez et al., 1990; Venkatesan et al., 1991; Echer et al., 2004): one is related to the transient phenomena, and another is related to recurrent high-speed solar wind streams. Different activities have different properties before arriving at the magnetosphere and will undergo different interaction processes with the magnetosphere and ionosphere. For example, Fig. 5 shows the scatter plots of (a) $\mathbf{ln}B$ against $\mathbf{ln}R_z$ and (b) $\mathbf{ln}aa$ against $\mathbf{ln}B$. One can see that the data points in Fig. 5a are all in between the two parallel (dashed) lines,

$$\begin{aligned} \mathbf{ln}B_t &= 1.51 + 0.14\mathbf{ln}R_z, \\ \mathbf{ln}B_b &= 1.16 + 0.14\mathbf{ln}R_z. \end{aligned} \tag{21}$$

The data points in Fig. 5b are all in between the two (dashed) lines,

$$\begin{aligned} \mathbf{ln}aa_t &= 0.10 + 1.77\mathbf{ln}B, \\ \mathbf{ln}aa_b &= -1.39 + 2.21\mathbf{ln}B. \end{aligned} \tag{22}$$

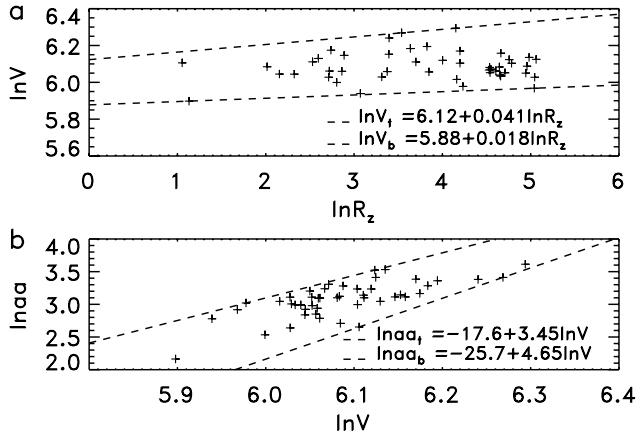

Fig. 6. **(a)** Scatter plot of $\mathbf{ln}V$ against $\mathbf{ln}R_z$ (pluses). The data points are all in between the two (dashed) lines of $\mathbf{ln}V_t$ (top) and $\mathbf{ln}V_b$ (base). **(b)** Scatter plot of $\mathbf{ln}aa$ against $\mathbf{ln}V$ (pluses). The data points are all in between the two (dashed) lines of $\mathbf{ln}aa_t$ (top) and $\mathbf{ln}aa_b$ (base).

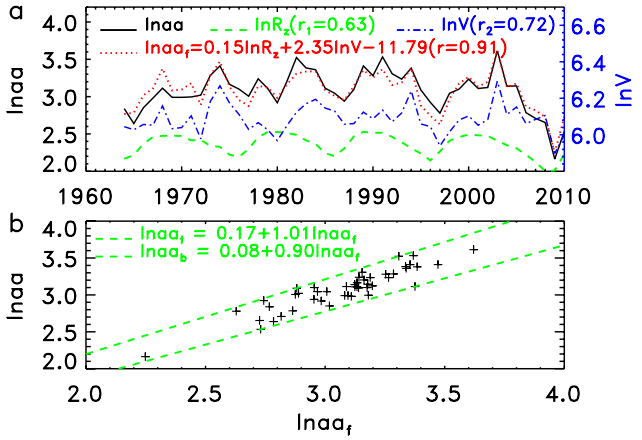

Fig. 7. **(a)** $\mathbf{ln}aa$ (solid), $\mathbf{ln}R_z$ (dashed), $\mathbf{ln}V$ (dash-dotted), and the fitted result $\mathbf{ln}aa_f$ (dotted) by the bivariate of $\mathbf{ln}R_z$ and $\mathbf{ln}V$. **(b)** Scatter plot of $\ln aa$ against $\ln aa_f$ (pluses). The data points are all in between the two (dashed) lines of $\mathbf{ln}aa_t$ (top) and $\mathbf{ln}aa_b$ (base).

As another example, Fig. 6 shows the scatter plots of (a) $\mathbf{ln}V$ against $\mathbf{ln}R_z$ and (b) $\mathbf{ln}aa$ against $\mathbf{ln}V$. One can also see that the data points in Fig. 6a are all in between the two (dashed) lines,

$$\begin{aligned} \mathbf{ln}V_t &= 6.12+0.041\mathbf{ln}R_z, \\ \mathbf{ln}V_b &= 5.88+0.018\mathbf{ln}R_z. \end{aligned} \tag{23}$$

The data points in Fig. 6b are all in between the two (dashed) lines,

$$\begin{aligned} \mathbf{ln}aa_t &= -17.6+3.45\mathbf{ln}V, \\ \mathbf{ln}aa_b &= -25.7+4.65\mathbf{ln}V. \end{aligned} \tag{24}$$

Now we analyze the bivariate-fit of $\mathbf{ln}aa$ (solid) to both $\mathbf{ln}R_z$ (dashed) and $\mathbf{ln}V$ (dash-dotted) from 1964 to 2010, as shown in Fig. 7a. The dotted line indicates the fitted result ($\mathbf{ln}aa_f$), with the regression equation given by

$$\mathbf{ln}aa = 0.15\mathbf{ln}R_z + 2.35\mathbf{ln}V - 11.79. \tag{25}$$

The correlation coefficient between $\mathbf{ln}aa$ and $\mathbf{ln}aa_f$ ($r = 0.91$) is slightly higher than ($r = 0.89$) between aa and the fitted result by the bivariate-fit of aa to both R_z and V.

Figure 7b shows the scatter plot of $\mathbf{ln}aa$ against $\mathbf{ln}aa_f$ (pluses). It is seen that the data points are all in between two (nearly parallel) lines,

$$\begin{aligned} \mathbf{ln}aa_t &= 0.17+1.01\mathbf{ln}aa_f, \\ \mathbf{ln}aa_b &= 0.08+0.90\mathbf{ln}aa_f. \end{aligned} \tag{26}$$

Therefore, the solar activity (R_z) is related to the solar winds (B, V) with values being in between two certain levels, and the solar winds (B, V) are related to the geomagnetic activities (aa) with values being in between another two certain levels. In turn, the solar activity (R_z) will be related to the geomagnetic activities (aa) that have a lowest and a highest level. Two ways can also be used to decompose an index (B, V, aa) into two components according the lowest or highest level of activity, as was the case in the previous section.

The above results imply that the source activities (B, V) of aa play a role of mid-processes in the formation of aa from solar magnetic field activity (R_z). These processes are similar to the relationship between aa and R_z discussed in the previous section. The results in Figs. 5a and 6a indicate that the source activities (B, V) have undergone decay processes before arriving at the magnetosphere (e.g., in the solar corona). The results in Figs. 5b and 6b indicate that the interactions of these activities with the magnetosphere and ionosphere will undergo further decays when generating aa. Generally speaking, the relationship between aa and R_z (Eq. 17) is the integrated effect of the above R_z-$B(V)$-aa (and R_z-CME-aa) relationships. Thus, the decay term (aa_d) should include the decays of solar winds (B, V), and the decay range (DR) may extend to the solar corona in this sense.

For ease of understanding, we discussed in Sect. 4.2 the decay process mainly in the magnetosphere and ionosphere. In Sect. 4.1, R_z is assumed to be associated with a certain amount of solar energy (E_t) potential of generating geomagnetic activity (aa). This statement is consistent with the suggestion that sunspots are related to the energy supply to the corona (de Toma et al., 2000; Temmer et al., 2003). The energy (E_t) should have been related to aa_t (or a similar formula) if there were no energy loss (E_d) in the decay processes or if E_d were all used to generate aa in the same way as the transient phenomena did.

However, it is not the case that all the solar energy (E_t) can generate or is directly related to geomagnetic activity (aa). The energy transmission from solar surface to the magnetosphere and ionosphere may involve very complex processes. One process (E_b) is associated with the transient phenomena

and follows the sunspot predominantly in a linear or nonlinear manner (aa_R or aa_b). Another process ($E_t - E_b$) is associated with other (recurrent) phenomena such as solar winds. The energy ($E_t - E_b = E_u + E_d$) for the latter process has undergone a loss (E_{d1}, part of E_d) before arriving at the magnetosphere and will undergo another loss ($E_{d2} = E_d - E_{d1}$) in the interactions with the magnetosphere and ionosphere. The energy loss (E_d) corresponds to the decay term (aa_d), which is related to solar (magnetic field) activity (R_z) because the energy ($E_t - E_b$) is associated with R_z as E_b is. It is shown in Sect. 4.2 that the decay aa_d precedes aa, which illustrates the fact that the generation of aa occurs after the decay (aa_d) or the energy loss (E_d). The energy E_u is the remainder of $E_t - E_b = E_u + E_d$ after the (decay) loss E_d. The geomagnetic activity (aa_u) generated by E_u is almost uncorrelated with aa_b, which is due to the various processes in the formation of both aa_b and aa_u.

The solar energy (E_t) can generate various solar activity phenomena such as solar flares, filament/prominence eruptions, energetic protons, CMEs, and solar winds (Gosling et al., 1976; Legrand and Simon, 1989a; Feminella and Storini, 1997; Sheeley et al., 1999; Forbes et al., 2006). These activities have lost part of their energies when passing over the solar chromospheric layer and corona. It is well known that most of these activities lag behind R_z from several months to a few years, which reflects the decay processes in the transmission. The energy loss (E_{d1}) for the decay process of one activity may generate other activities, including various electric-magnetic radiations and the variations in density and temperature of the solar chromospheric layer and corona. Therefore, most solar activities are well correlated with R_z (or E_t), which is the reason for the good correlation of aa_d with R_z. The relationships between these activities and R_z are similar to that between aa and R_z before arriving at the magnetosphere, as can be seen in Figs. 5a and 6a for two examples of the B-R_z and V-R_z relationships, respectively.

Similarly, the interactions of the source activities with the magnetosphere and ionosphere can also generate a series of activity phenomena such as the ring current, auroral current, and the variations in density and temperature of the Earth's atmosphere. The energy loss (E_{d2}) for the decay process of one activity may generate other activities, and not all these activities are completely related to aa. The relationships between aa and these activities are similar to that between aa and R_z, as shown in Figs. 5b and 6b for two examples of the aa-B and aa-V relationships, respectively. In summary, aa is the synthesis effect of all the above processes.

The main points of this paper may be summarized as follows:

1. The aa index is in between the two levels of $aa_t = e^{2.44} R_z^{2/7}$ and $aa_b = e^{1.36} R_z^{2/7}$.

2. aa can be decomposed into two independent components: $aa = aa_b + aa_u$ ($r = 0.09$). aa_t can be divided into two independent terms: $aa_t = aa + aa_d$ ($r = 0.00$).

3. All the aa values can be expressed as $aa = aa_t - aa_d = e^{2.44 \pm 0.05 - \eta} R_z^{2/7 \pm 0.02}$ for $0 \le \eta \le 1.08$, where η refers to the "decay index", modulated mainly by the solar wind speed.

Acknowledgements. The authors are grateful to the anonymous referees for suggestive comments, which greatly improved the present manuscript. This work is supported by the National Natural Science Foundation China through grants 10973020, 40890161, and 10921303, Chinese Academy of Sciences through grant YYYJ-1110, and National Basic Research Program of China through grant 2011CB811406.

Topical Editor R. Nakamura thanks J. Lei and another anonymous referee for their help in evaluating this paper.

References

Bame, S. J., Asbridge, J. R., Feldman, W. C., and Gosling, J. T.: Solar cycle evolution of high-speed solar wind streams, Astrophys. J., 207, 977–980, 1976.

Crooker, N. U., Feynman, J., and Gosling, J. T.: On the high correlation between long-term averages of solar wind speed and geomagnetic activity, J. Geophys. Res., 82, 1933–1937, 1977.

Demetrescu, C. and Dobrica, V.: Signature of Hale and Gleissberg solar cycles in the geomagnetic activity, J. Geophys. Res., 113, A02103, doi:10.1029/2007JA012570, 2008.

de Toma, G., White, O. R., and Harvey, K. L.: A Picture of Solar Minimum and the Onset of Solar Cycle 23. I. Global Magnetic Field Evolution, Astrophys. J., 529, 1101–1114, 2000.

Du, Z. L.: The Relationship between Prediction Accuracy and Correlation Coefficient, Solar. Phys., 270, 407–416, 2011a.

Du, Z. L.: The correlation between solar and geomagnetic activity – Part 2: Long-term trends, Ann. Geophys., Ann. Geophys., 29, 1341–1348, doi:10.5194/angeo-29-1341-2011, 2011b.

Du, Z. L.: The correlation between solar and geomagnetic activity – Part 3: An integral response model, Ann. Geophys., 29, 1005–1018, doi:10.5194/angeo-29-1005-2011, 2011c.

Du, Z. L., Li, R., and Wang, H. N.: The Predictive Power of Ohl's Precursor Method, Astron. J., 138, 1998–2001, 2009.

Echer, E., Gonzalez, W. D., Gonzalez, A. L. C., Gonzalez, W. D., Gonzalez, A. L. C., Prestes, A., Vieira, L. E. A., Dal Lago, A., Guarnieri, F. L., and Schuch, N. J.: Long-term correlation between solar and geomagnetic activity, J. Atmos. Sol. Terr. Phys., 66, 1019–1025, 2004.

Feminella, F. and Storini, M.: Large-scale dynamical phenomena during solar activity cycles, Astron. Astrophys., 322, 311–319, 1997.

Feynman, J.: Implications of solar cycles 19 and 20 geomagnetic activity for magnetospheric processes, Geophys. Res. Lett., 7, 971–973, 1980.

Feynman, J.: Geomagnetic and solar wind cycles, 1900–1975, J. Geophys. Res., 87, 6153–6162, 1982.

Feynman, J.: Reply, J. Geophys. Res., 88, 8139–8140, 1983.

Feynman, J. and Crooker, N. U.: The solar wind at the turn of the century, Nature, 275, 626–627, 1978.

Forbes, T. G., Linker, J. A., Chen, J., Cid, C., Kota, J., Lee, M. A., Mann, G., Mikic, Z., Potgieter, M. S., Schmidts, J. M., Siscoe, G. L., Vainio, R., Antiochos, S. K., and Riley, P.: CME Theory and Models, Space Sci. Rev., 123, 251–302, 2006.

Garrett, H. B., Dessler, A. J., and Hill, T. W.: Influence of solar wind variability on geomagnetic activity, J. Geophys. Res., 79, 4603–4610, 1974.

Gonzalez, W. D., Gonzalez, A. I. C., and Tsurutani, B. T.: Dual-peak solar cycle distribution of intense geomagnetic storms, Planet. Space Sci., 38, 181–187, 1990.

Gosling, J. T., Hildner, E., MacQueen, R. M., Munro, R. H., Poland, A. I., and Ross, C. L.: The speeds of coronal mass ejection events, Solar Phys., 48, 389–397, 1976.

Hathaway, D. H. and Wilson, R. M.: Geomagnetic activity indicates large amplitude for sunspot cycle 24, Geophys. Res. Lett., 33, L18101, doi:10.1029/2006GL027053, 2006.

Johnson, J. R. and Wing, S.: A solar cycle dependence of nonlinearity in magnetospheric activity, J. Geophys. Res., 110, A04211, doi:10.1029/2004JA010638, 2005.

Leamon, R. J., Matthaeus, W. H., Smith, C. W., Zank, G. P., Mullan, D. J., and Oughton, S.: MHD-driven Kinetic Dissipation in the Solar Wind and Corona, Astrophys. J., 537, 1054–1062, 2000.

Legrand, J. P. and Simon, P. A.: Ten cycles of solar and geomagnetic activity, Solar Phys., 70, 173–195, 1981.

Legrand, J. P. and Simon, P. A.: Comment on 'geomagnetic and solar wind cycles, 1900–1975' by Joan Feynman, J. Geophys. Res., 88, 8137–8138, 1983.

Legrand, J. P. and Simon, P. A.: Solar cycle and geomagnetic activity: A review for geophysicists. I – The contributions to geomagnetic activity of shock waves and of the solar wind, Ann. Geophys., 7, 565–578, 1989a.

Legrand, J. P. and Simon, P. A.: Solar cycle and geomagnetic activity: A review for geophysicists. II – The solar sources of geomagnetic activity and their links with sunspot cycle activity, Ann. Geophys.,7, 579–593, 1989b.

Li, Y.: Predictions of the features for sunspot cycle 23, Sol. Phys., 170, 437–445, 1997.

Lukianova, R., Alekseev, G., and Mursula, K.: Effects of station relocation in the aa index, J. Geophys. Res., 114, A02105, doi:10.1029/2008JA013824, 2009.

Matthaeus, W. H., Weygand, J. M., Chuychai, P., Dasso, S., Smith, C. W., and Kivelson, M. G.: Interplanetary Magnetic Taylor Microscale and Implications for Plasma Dissipation, Astrophys. J. Lett., 678, L141–L144, 2008.

Mayaud, P. N.: The aa indices: A 100-year series characterizing the magnetic activity, J. Geophys. Res., 77, 6870–6874, 1972.

Nagashima, K., Fujimoto, K., and Tatsuoka, R.: Nature of solar-cycle and heliomagnetic-polarity dependence of cosmic rays, inferred from their correlation with heliomagnetic spherical surface harmonics in the period 1976–1985, Planet. Space Sci., 39, 1617–1635, 1991.

Nevanlinna, H. and Kataja, E.: An extension of the geomagnetic activity index series aa for two solar cycles (1844–1868), Geophys. Res. Lett., 20, 2703–2706, 1993.

Papitashvili, V. O., Papitashvili, N. E., and King, J. H.: Solar cycle effects in planetary geomagnetic activity: Analysis of 36-year long OMNI dataset, Geophys. Res. Lett., 27, 2797–2800, 2000.

Richardson, I. G., Cliver, E. W., and Cane, H. V.: Sources of geomagnetic activity over the Solar cycle: relative importance of coronal mass ejections, high-speed streams, and slow Solar wind, J. Geophys. Res., 105, 18203–18213, 2000.

Russell, C. T. and McPherron, R. L.: Semiannual variation of geomagnetic activity, J. Geophys. Res., 78, 92–108, 1973.

Schatten, K. H., Scherrer, P. H., Svalgaard, L., and Wilcox, J. M.: Using dynamo theory to predict the sunspot number during solar cycle 21, Geophys. Res. Lett., 5, 411–414, 1978.

Sheeley, N. R., Walters, J. H., Wang, Y.-M., and Howard, R. A.: Continuous tracking of coronal outflows: Two kinds of coronal mass ejections, J. Geophys. Res., 104, 24739–24768, 1999.

Simon, P. A. and Legrand, J. P.: Solar cycle and geomagnetic activity: A review for geophysicists. II – The solar sources of geomagnetic activity and their links with sunspot cycle activity, Ann. Geophys.,7, 579–593, 1989.

Snyder, C. W., Neugebauer, M., and Rao, U. R.: The Solar Wind Velocity and Its Correlation with Cosmic-Ray Variations and with Solar and Geomagnetic Activity, J. Geophys. Res., 68, 6361–6370, 1963.

Stamper, R., Lockwood, M., Wild, M. N., and Clark, T. D. G.: Solar causes of the long-term increase in geomagnetic activity, J. Geophys. Res., 104, 28325–28342, 1999.

Svalgaard, L.: Geomagnetic activity: Dependence on solar wind parameters, in: Coronal Holes and High Speed Wind Streams, edited by: Zirker, J. B., Colorado Ass. U. Press, Boulder, p. 371, 1977.

Temmer, M., Veronig, A., and Hanslmeier, A.: Does solar flare activity lag behind sunspot activity? Sol. Phys., 215, 111–126, 2003.

Tsurutani, B. T., Gonzalez, W. D., Gonzalez, A. L. C., Guarnieri, F. L., Gopalswamy, N., Grande, M., Kamide, Y., Kasahara, Y., Lu, G., Mann, I., McPherron, R., Soraas, F., and Vasyliunas, V.: Corotating solar wind streams and recurrent geomagnetic activity: A review, J. Geophys. Res., 111, A07S01, doi:10.1029/2005JA011273, 2006.

Tu, C. Y. and Marsch, E.: MHD structures, waves and turbulence in the solar wind: observations and theories, Space Sci. Rev., 73, 1–210, 1995.

Venkatesan, D., Shulka, A. K., and Agrawal, S. P.: Cosmic ray intensity variations and two types of high speed soalr streams, Solar Phys., 81, 375–381, 1982.

Venkatesan, D., Ananth, A. G., Graumann, H., and Pillai, S.: Relationship between solar and geomagentic activity, J. Geophys. Res., 96, 9811–9813, 1991.

Wang, Y. M. and Sheeley, N. R.: Understanding the Geomagnetic Precursor of the Solar Cycle, Astrophys. J., 694, L11–L15, 2009.

Wilson, R. M.: On the level of skill in predicting maximum sunspot number – A comparative study of single variate and bivariate precursor techniques, Solar Phys., 125, 143–155, 1990.